Proceedings of the 4th International Conference on Functional Materials and Civil Engineering
DOI: 10.54254/2755-2721/2026.36407

Multi-Objective Build-Orientation Optimisation for Support-Structure Reduction in Additive Manufacturing

Jiaman Ding

Ordos No.1 Middle School (East Campus), Ordos, China
18204926660@163.com

Abstract. Support structures in additive manufacturing consume additional material and build time, and damage the contact surface after removal. The build orientation determines which surfaces become overhangs before slicing, and is the lowest-cost intervention point, but the orientation space is continuous and the objective is highly non-convex, so neither the default orientation nor grid trial placements can reliably locate the optimal region. This paper expresses build-orientation selection as a bi-objective optimisation problem of support volume and build height, solved by a multi-start NSGA-II with axis-seeded initialisation and compared against area-uniform spherical grid enumeration at a matched evaluation budget on 120 real printable models from Thingi10K. Among the 84 models that require support under the as-uploaded orientation, optimisation reduced the median support volume by 69.0% (interquartile range 3.5% to 97.4%, $p<0.001$), while 16 models did not improve, so the benefit depends strongly on the specific geometry. With the grid given slightly more evaluations, the normalised hypervolume of NSGA-II was no less than that of the grid on 112 models ($p<0.001$). The two objectives were negatively correlated within all fronts, so the trade-off genuinely exists. The reduction is sensitive to the critical overhang angle: at 60° the median reduction is only 1.4%. This paper gives a budget-matched comparison protocol and quantifies the applicable boundary of the method's benefit.

Keywords: additive manufacturing, build orientation, support structure, multi-objective optimisation, NSGA-II

1. Introduction

Additive manufacturing processes such as material extrusion and powder bed fusion build up layer by layer. When the angle between a surface and the build platform falls below the critical value allowed by the process, that surface lacks solidified material beneath it and a support structure must be printed first. Support carries a triple cost: additional material, longer build time, and rough traces left on the contact surface after removal. Recent reviews of support-free printing for powder bed fusion [1] and of overhang fabrication defects [2] reflect the fundamental status of the problem in the process chain.

Among the variables affecting the amount of support, the build orientation holds a special position: it is fixed before slicing and changes neither the part geometry nor the process sequence, yet it directly determines which surfaces fall under the overhang criterion. Adjusting support

DOI: 10.54254/2755-2721/2026.36407

parameters only optimises support already generated, and modifying the geometry involves functional and strength verification; both cost more.

Orientation selection in practice is limited. Most users adopt the orientation that comes with the model; more careful users try several postures manually or evaluate a set of discrete orientations. Both share the assumption that a good orientation can be found in a few trials. But the feasible domain is a continuous unit sphere and the support volume is not smooth in the orientation: a small rotation can push a large area across the overhang criterion, making the support amount jump. On such a landscape, sparse sampling routinely misses the optimal region.

Existing studies verify their methods on few examples, and the evaluation budget of the comparison is often unequal, so algorithm advantage cannot be separated from budget advantage. This paper contributes three things. First, build-orientation selection is formalised as a bi-objective problem of support volume and build height and solved on 120 real printable models, stratified by face count over about two orders of magnitude of geometric complexity. Second, a budget-matched protocol gives the grid no fewer evaluations than the evolutionary algorithm, so the conclusion does not rest on a budget difference. Third, the benefit is reported across critical overhang angles, identifying where it narrows sharply.

2. Literature review

Research on build-orientation optimisation has long revolved around the choice of objective, shifting from a single indicator to several treated concurrently. Darvishi et al. [3] optimised surface roughness, build time and mechanical properties together, showing that these indicators restrain each other along the orientation dimension; Birosz et al. [4] introduced principal stress lines into joint shape and orientation optimisation for material extrusion. The objective set has since expanded to thermal behaviour: Wang et al. [5] optimise orientation against thermal distortion, González et al. [6] proposed a temperature index for powder bed fusion, and Haveroth et al. [7] used a thermal model to treat support design and orientation together. The influence of orientation is thus not limited to the geometric level.

Another route eliminates the support need at the design stage by introducing self-supporting constraints into topology optimisation, so that the structure satisfies the overhang criterion in a given orientation. Xu et al. [8] combined self-supporting topology optimisation with curved layer slicing for multi-axis processes, Shin et al. [9] treated overhang and material anisotropy together, Guo et al. [10] validated three-dimensional self-supporting structures and printing paths, and Nti et al. [11] proposed support-free topography slicing for three-axis material extrusion. Such work changes the geometry or the kinematics, whereas this paper keeps the geometry fixed and adjusts only the placement posture.

The two lines converge in joint topology and orientation optimisation. Crispo and Kim [12] considered build height and overhang area together, then incorporated support minimisation into the same framework [13], confirming a structural conflict between build height and overhang amount that motivates the objectives used here. Support geometry itself can also be optimised: Nasr et al. [14] improved block supports for the electron beam process with machine learning-driven multi-objective optimisation, indicating that support geometry and orientation can be handled in separate layers.

Multi-objective evolutionary algorithms are widely used at the algorithm level because one run yields the whole trade-off curve. NSGA-II [15] remains a common benchmark through its fast non-dominated sorting and crowding distance mechanism. Günaydın and Yıldız [16] compared several

DOI: 10.54254/2755-2721/2026.36407

recent algorithms on the build-orientation problem, and Bacciaglia et al. [17] proposed an efficient industrial part orientation algorithm aimed at solution speed rather than solution quality alone.

Two gaps remain. Most methods are validated on at most a few dozen examples of limited geometric diversity, and comparisons between algorithms rarely control the evaluation budget, which is the dominant computational expense here. This paper addresses both with a real model benchmark and a budget-matched protocol.

3. Methodology

3.1. Problem formulation

Let the build orientation be the unit vector d, parameterised by the spherical polar angle θ and the azimuth angle ϕ :

$$d(\theta,\phi)=(\sin\theta\cos\phi,\ \sin\theta\sin\phi,\ \cos\theta) \tag{1}$$

where $\theta\in[0,\pi]$ and $\phi\in[0,2\pi)$. For a triangular face f, let its unit outward normal be n_f, its area be A_f, and its centroid be c_f. When the angle between the face and the build platform plane is less than the critical overhang angle α, support is required. This condition is equivalent to the angle between the outward normal and $-d$ being less than α :

$$n_f\cdot d<-\cos\alpha \tag{2}$$

Let the set of faces satisfying Eq. (2) be S. The support volume is estimated by vertical projection columns, that is, each overhang face is projected onto the build platform along the $-d$ direction, the cross-section of the column is the projected area of the face, and the height is the distance from the centroid to the lowest point of the model:

$$V_s=\sum_{f\in S}A_f|n_f\cdot d|(c_f\cdot d-h_{\min}) \tag{3}$$

where $h_{\min}=\min_v(v\cdot d)$ is the minimum projection of all vertices along the build orientation. The build height is the span of the vertex projections, which determines the number of layers and is therefore the main driver of build time:

$$H_b=\max_v(v\cdot d)-h_{\min} \tag{4}$$

The optimisation problem is to find the Pareto-optimal set of the two objectives on the sphere:

DOI: 10.54254/2755-2721/2026.36407

$$\min_{\theta,\phi} \left(V_s(\theta,\phi),\ H_b(\theta,\phi)\right) \tag{5}$$

The critical overhang angle is fixed at the industrial default of 45°, and is treated as a process constraint rather than a decision variable. Lowering this angle would classify surfaces that actually require support as self-supporting, which is a build failure rather than an optimisation benefit.

3.2. Benchmark dataset

The experimental data are taken from Thingi10K, which collects models actually used for three-dimensional printing and is therefore uneven in geometric quality, making it suitable for testing a method on real input. A printable subset was screened from its official geometric metadata: vertex- and edge-manifold, consistently oriented, no boundary edges, no self-intersections, solid with a piecewise-constant winding number, a single connected component, and 1000 to 60000 faces. Out of 9997 models, 2580 meet all conditions. From this pool, 120 models were sampled in equal numbers stratified by face-count quartile, with a median face count of 4571 ranging from 1022 to 54006, so that no single complexity interval dominates the conclusion.

3.3. Solution method and control

The solution adopts a multi-start NSGA-II [15]. The initial population contains the orientation that comes with the model and the six coordinate-axis directions, with the remaining individuals drawn area-uniformly on the sphere, that is, $\cos\theta$ rather than θ is uniform. Seeding makes the starting point no worse than any conventional placement, so the conclusion that optimisation beats the baseline does not rest on the luck of random initialisation. One run uses a population of 60 over 30 generations; three independent restarts are merged, giving 5400 objective evaluations. Multiple restarts are necessary because the objective is highly non-convex and the optimal region may occupy only a small patch of the sphere, which a single run often misses.

The control is area-uniform grid enumeration over 52×104, a total of 5408 directions, so the grid receives slightly more evaluations than the evolutionary algorithm. The reference front is the non-dominated set of an independent 60×120 dense grid together with the output of both methods and the baseline; it belongs to no single method and serves only as a common ruler for convergence.

3.4. Statistical methods

Support volume spans five orders of magnitude across samples and is highly right-skewed, so it is described by the median and interquartile range, paired comparisons use the Wilcoxon signed-rank test, and effect sizes are reported as rank-biserial correlations. Models with a baseline support volume below 1 cubic millimetre are treated as requiring no support in engineering terms; the relative reduction is undefined there, so support reduction is computed only on the subset that requires support. All experiments ran under a fixed random seed and reproduced on rerun.

DOI: 10.54254/2755-2721/2026.36407

4. Results

4.1. Baseline characterisation

Under the as-uploaded orientation, 84 (70.0%) of the 120 models require support, and the bottom faces of the remaining 36 essentially sit flat on the build platform. The median support volume of the subset that requires support is 1250.8 cubic millimetres, and the interquartile range is 183.8 to 8439.4. The median build height over the whole sample is 20.0 mm, and the median ratio of overhang area to total surface area is 0.178.

4.2. Reduction in support volume

On the 84 models that require support, the optimised orientation reduces the median support volume by 69.0%, with an interquartile range of 3.5% to 97.4% (Wilcoxon signed-rank test, $p<0.001$, rank-biserial correlation coefficient 0.992). The improvement appeared on 68 models (81.0%), and the as-uploaded orientation of the other 16 models was already support-optimal, so optimisation could not reduce it further. Individual differences are extremely large, and the lower bound of the interquartile range is only 3.5%, indicating that the median cannot represent all cases.

The reduction remains stable across different complexity ranges. Splitting the face count into three equal groups, the median reduction of the low, middle and high groups was 74.4%, 74.7% and 51.2% respectively, and all three groups were significant ($p<0.001$). No significant association was found between the reduction and the baseline overhang area ratio (Spearman rank correlation coefficient −0.209, $p=0.056$).

The minimum-support solution is not without cost: the median change in the build height is 0.0%, but 41 out of 84 models have an increased build height. Standing the part upright can often reduce overhang and raise the build height at the same time.

4.3. Budget-matched comparison of algorithm efficiency

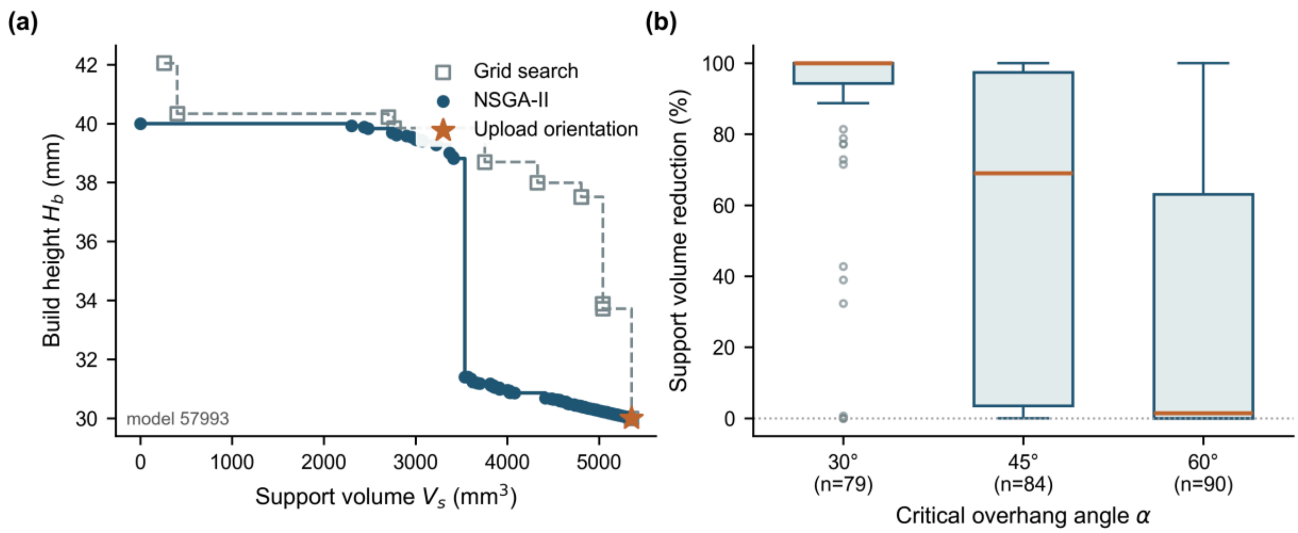

Figure 1. Main results

With the grid at 5408 evaluations and the evolutionary algorithm at 5400, the median normalised hypervolume relative to the reference front is 1.0000 for NSGA-II and 0.9461 for the grid ($p<0.001$,

DOI: 10.54254/2755-2721/2026.36407

rank-biserial correlation coefficient 0.846). NSGA-II is no worse than the grid on 112 models (93.3%); the grid is better on the remaining 8. On the minimum-support solution the grid falls short on 51 models (60.7%), with a median shortfall of 4.5%. Median front size is 3.0 against 2.0 for the grid. Figure 1(a) shows the difference on a representative model, and Table 1 compares the three methods.

Table 1. Summary of comparative results

Metric	Upload orientation	Grid search	NSGA-II
Evaluations per model	1	5408	5400
Median support volume (mm^3)	1250.8	329.8	178.1
Median hypervolume ratio	0.110	0.946	1.000
Median Pareto front size	1	2	3
Best support minimum attained	—	39.3%	100%

Support volume is reported on the 84 models requiring support at the upload orientation; hypervolume is normalised against the common reference front. The last row is the share of those models on which the method reached the lower minimum-support solution.

The baseline orientation is dominated by some solution on the front on 71 models (59.2%), that is, there exists an orientation that is simultaneously no worse than the baseline (binomial test $p=0.027$). If the equal-weight compromise knee solution is adopted, only 22 models (26.2%) are better than the baseline on both objectives at the same time, indicating that win-win solutions are not universal.

4.4. Trade-off structure and convergence stability

On the fronts with no fewer than four points, the median Spearman rank correlation coefficient between the support volume and the build height is −1.0, and all fronts are negative ($p<0.001$), so the two objectives genuinely conflict within the solution set. Three independent restarts obtained a consistent minimum-support value on 50.8% of the models, and there are differences in the rest, which supports the multi-start setting. The total computation of a single model takes an average of 2.37 seconds.

4.5. Robustness

When the critical overhang angle is 30°, 45° and 60°, the number of models requiring support is 79, 84 and 90 respectively, and the median reduction is 100.0%, 69.0% and 1.4% respectively, all of which are significant ($p<0.001$). The statistical significance holds under all three values, but the magnitude of the benefit narrows sharply as the angle increases, as shown in Figure 1(b).

The projection approximation of the support volume is highly consistent with the occlusion-aware ray-casting exact value (Spearman rank correlation coefficient 0.972, $p<0.001$), and the median ratio of the exact value to the approximate value is 0.791, that is, the approximation systematically overestimates the absolute support amount by about a quarter. Recalculated with exact values, the median support reduction is 63.6%, and the direction of the conclusion remains unchanged ($p<0.001$).

DOI: 10.54254/2755-2721/2026.36407

5. Discussion

The results support a bounded conclusion: at the industrial default overhang angle, orientation optimisation significantly reduces support volume on most models that require support, but the benefit is distributed very unevenly. The 3.5% lower quartile and the 16 models without improvement show that some as-uploaded orientations are already close to support-optimal, consistent with designers straightening parts before uploading. Treating the method as a routine step in the process chain is reasonable; treating the median reduction as the expected benefit for a single part is not.

The algorithm comparison points to how the budget is spent rather than how large it is. A uniform grid spreads evaluations over the entire sphere, while the optimal region is often confined to a narrow angular range that uniform sampling rarely lands in; the evolutionary algorithm concentrates the budget generation by generation into promising regions and so returns a more complete front at the same cost. The gap widens with the ruggedness of the landscape, which also explains the 8 models on which the grid is better: where the landscape is relatively flat, uniform coverage costs nothing.

The sensitivity to the critical overhang angle matters directly in practice. At 60° the median reduction drops to 1.4%; it remains statistically significant but no longer carries practical value, because the criterion is then strict enough that most inclined surfaces require support and rotating the part gains little. Where equipment and material allow a smaller critical angle, orientation optimisation pays off more; otherwise the effort is better spent on support geometry or part design.

The projection approximation does not deduct the part of the column path occupied by solid material and so systematically overestimates the absolute amount; the ray-casting check reaches a rank correlation of 0.972 and leaves the conclusion unchanged, so the approximation supports ranking between orientations but not prediction of actual material consumption. Build height as a proxy for build time ignores differences in per-layer scanning path length. The conclusion is limited to geometric support amount and height, and does not cover the influence of orientation on mechanical properties, surface roughness and thermal distortion, which are also orientation-dominated [3, 5]. The benchmark is a consumer-grade model library, so transfer to large industrial parts requires separate verification.

6. Conclusion

This paper expresses build-orientation selection as a bi-objective optimisation problem of support volume and build height, solved by a multi-start NSGA-II with axis-seeded initialisation and compared against area-uniform grid enumeration at a matched evaluation budget on 120 real printable models from Thingi10K.

Three findings follow. First, among the 84 models requiring support under the as-uploaded orientation, optimisation reduced the median support volume by 69.0% and improved 81.0% of them, but the interquartile range spans 3.5% to 97.4%, so the benefit depends strongly on the specific geometry. Second, with the grid given slightly more evaluations, evolutionary search returned a front no worse than enumeration on 112 models (93.3%), a difference that comes from how the budget is allocated rather than its total. Third, the two objectives are negatively correlated within all fronts, so the trade-off genuinely exists, and the equal-weight compromise solution beats the baseline on only 26.2% of the models.

The benefit boundary is equally clear: raising the critical overhang angle from 45° to 60° drops the median reduction from 69.0% to 1.4%, leaving orientation optimisation close to ineffective

DOI: 10.54254/2755-2721/2026.36407

under a strict criterion. This study is exploratory and was not pre-registered; all results are reported as they are, including the models without improvement and the cases where the grid prevailed. Follow-up work can add surface roughness and thermal distortion to the objective set and test transferability on industrial-scale parts.

Declaration of interest

The author declares no conflict of interest.

Author contribution

The author confirms sole responsibility for study conception and design, data collection, analysis and interpretation of results, and manuscript preparation.

References

[1] Hajnys, J., Ma, Q. P., Vandzura, R., et al. (2026). A review on support-free printing with powder bed fusion method. *Progress in Additive Manufacturing, 11*(1), 717-733. https://doi.org/10.1007/s40964-025-01373-1

[2] Cong, S., Gu, H., Wei, C., et al. (2025). Advancements and challenges in overhang structure fabrication during laser powder bed fusion: A comprehensive review. *Virtual and Physical Prototyping, 20*(1), e2567382. https://doi.org/10.1080/17452759.2025.2567382

[3] Darvishi, I., Khodaygan, S., Mohammadi, K., et al. (2023). Concurrent optimization of surface roughness, build time, and mechanical properties of additively manufactured product in terms of part build orientation. *Progress in Additive Manufacturing, 8*(6), 1455-1471. https://doi.org/10.1007/s40964-023-00413-y

[4] Birosz, M. T., Safranyik, F., & Andó, M. (2023). Concurrent shape and build orientation optimization for FDM additive manufacturing using the principal stress lines (PSL). *Heliyon, 9*(4), e15022. https://doi.org/10.1016/j.heliyon.2023.e15022

[5] Wang, W., Li, S., Yang, L., et al. (2024). Build orientation optimization considering thermal distortion in additive manufacturing. *Computer Aided Geometric Design, 114*, 102393. https://doi.org/10.1016/j.cagd.2024.102393

[6] González, A., Barea, R., & Corbera, S. (2025). A new temperature index for build orientation optimization in powder bed fusion additive manufacturing. *Additive Manufacturing, 99*, 104660. https://doi.org/10.1016/j.addma.2025.104660

[7] Haveroth, G. A., Thore, C. J., Ausas, R. F., et al. (2024). A thermal model for topology optimization in additive manufacturing: Design of support structures and geometry orientation. *Computers & Structures, 301*, 107453. https://doi.org/10.1016/j.compstruc.2024.107453

[8] Xu, S., Liu, J., He, D., et al. (2025). Self-support structure topology optimization for multi-axis additive manufacturing incorporated with curved layer slicing. *Computer Methods in Applied Mechanics and Engineering, 438*, 117841. https://doi.org/10.1016/j.cma.2025.117841

[9] Shin, S., Goh, B., Oh, Y., et al. (2025). Topology optimization for multi-axis additive manufacturing considering overhang and anisotropy. *International Journal of Mechanical Sciences, 301*, 110443. https://doi.org/10.1016/j.ijmecsci.2025.110443

[10] Guo, Q., Ye, J., Lu, H., et al. (2024). Design and validation of 3D self-supporting structures and printing paths for multi-axis additive manufacturing. *Additive Manufacturing, 96*, 104563. https://doi.org/10.1016/j.addma.2024.104563

[11] Nti, J., Tucker, M., Bambach, M., et al. (2026). Automated topography slicing for support-free 3-axis FDM. *The International Journal of Advanced Manufacturing Technology*. https://doi.org/10.1007/s00170-026-18768-1

[12] Crispo, L., & Kim, I. Y. (2024). Topology and build orientation optimization for additive manufacturing considering build height and overhang area. *Structural and Multidisciplinary Optimization, 67*(6), 98. https://doi.org/10.1007/s00158-024-03808-9

[13] Crispo, L., & Kim, I. Y. (2025). Combined topology and build orientation optimization for support structure minimization in additive manufacturing. *Structural and Multidisciplinary Optimization, 68*(10), 216. https://doi.org/10.1007/s00158-025-04124-6

[14] Nasr, M. M., Ameen, W., & Dabwan, A. et al. (2025). Machine learning-based multi-objective optimization for enhancing the performance of block support structures for electron beam additive manufacturing. *Metals, 15*(6),

671. https://doi.org/10.3390/met15060671

[15] Deb, K., Pratap, A., & Agarwal, S. et al. (2002). A fast and elitist multiobjective genetic algorithm: NSGA-II. *IEEE Transactions on Evolutionary Computation, 6*(2), 182-197. https://doi.org/10.1109/4235.996017

[16] Günaydın, A. C., & Yıldız, A. R. (2024). A comparison of recent optimization algorithms for build orientation problems in additive manufacturing. *Materials Testing, 66*(10), 1539-1556. https://doi.org/10.1515/mt-2024-0099

[17] Bacciaglia, A., Liverani, A., & Ceruti, A. (2024). Efficient part orientation algorithm for additive manufacturing in industrial applications. *The International Journal of Advanced Manufacturing Technology, 133*(11-12), 5443-5462. https://doi.org/10.1007/s00170-024-14039-z